Arch. Pharm. Res. (2017) 40:864–874
DOI 10.1007/s12272-017-0930-1

Online ISSN 1976-3786
Print ISSN 0253-6269

Archives of Pharmacal Research
www.springer.com/12272

RESEARCH ARTICLE

Ginsenoside improves physicochemical properties and bioavailability of curcumin-loaded nanostructured lipid carrier

Ajay Vijayakumar[1] · Rengarajan Baskaran[1] · Han-Joo Maeng[1] · Bong Kyu Yoo[1]

Received: 7 February 2017 / Accepted: 12 July 2017 / Published online: 15 July 2017

Abstract The aim of this study was to develop a ginsenoside-modified nanostructured lipid carrier (G-NLC) dispersion containing curcumin. The NLC was prepared by melt emulsification with slight modification process. Different G-NLC dispersion systems were prepared using lipid carrier matrix composed of ginsenoside, phosphatidylcholine, lysophosphatidylcholine, and hydrogenated bean oil. TEM image of the nanoparticles in the NLC dispersion showed core/shell structure, and there was corona-like layer surrounding the particles in the G-NLC. The mean particle size of G-NLC dispersion was in the range of about 300–500 nm and stayed submicron size up to 12 months. The in vitro release of curcumin was faster in pH 1.2 compared to pH 6.8 and it showed linear release pattern after lag time of 1 h. When the G-NLC dispersion was orally administered to rats, C_{max} of the free curcumin was 15.2 and 32.3 ng/mL at doses of 50 and 100 mg/kg, respectively, while it was below quantification limit when curcumin was administered as of dispersion in distilled water. Based on these results, it is certain that ginsenoside modulated the NLC dispersion, leading to enduring shelf-life of the dispersion system and enhanced bioavailability. These results strongly suggest that ginsenoside holds a promising potential as a pharmaceutical excipient in the pharmaceutical industries to increase the utility of various bioactives.

✉ Bong Kyu Yoo
byoo@gachon.ac.kr

[1] Gachon Institute of Pharmaceutical Sciences, Gachon University, 191 Hambakmoero, Yeonsu-gu, Incheon 21936, Republic of Korea

Keywords Ginsenoside · Curcumin · Nanostructured lipid carrier · Stability · Bioavailability

Introduction

Ginsenosides are a group of naturally occurring dammarane-type steroid glycosides, and there have been extensive studies on the pharmacological activity of the ginsenosides, which include anti-stress, anti-inflammation, and anti-cancer effects (Byeon et al. 2009; Kim et al. 2012; Piao et al. 2013; Zhang et al. 2013). Ginsenosides have sugar moiety (mainly glucose) attached to the steroid skeleton, so they are amphiphilic compounds in nature. Therefore, ginsenosides can be used as pharmaceutical excipients to enhance the bioavailability of bioactives with low solubility and permeability. However, the potential use of ginsenosides as such has not yet been explored in the pharmaceutical industry.

Curcumin is a hydrophobic polyphenol compound derived from the rhizome of turmeric (*Curcuma longa*) plant, a perennial herb of the ginger family, that is used for food coloring and flavoring in private and commercial setting. Numerous researches have been carried out so far to take advantage of its antioxidant, anti-inflammatory, and anticancer properties (Menon and Sudheer 2007; Wang et al. 2012; Anuchapreeda et al. 2012; Du et al. 2013). Despite the promising benefits, however, it has not been successful in exploiting the anticipated activities of curcumin in the treatment of various diseases mainly owing to its low bioavailability (Goel and Aggarwal 2010; Prasad et al. 2014). Reasons for the low bioavailability include low solubility, poor gastrointestinal tract absorption, rapid metabolism, and rapid excretion from the body.

A range of approaches have been empolyed to enhance the bioavailability of curcumin using formulation technologies such as liposomes, nanoparticles, solid lipid nanoparticles, nanostructured lipid carriers (NLC), mixed micelles, and phospholipid complexes (Arun et al. 2012; Kumar et al. 2014; Popat et al. 2014; Udompornmongkol and Chiang 2015; Tabatabaei Mirakabad et al. 2016). Among the formulations developed, phospholipid complexes appear to be successfully launched in the global market (Meriva^{TM} and Longvida^{TM}). However, the extent of bioavailability enhancement achieved by the phospholipid complexes remains controversial because levels of the physiologically active form (free curcumin) were extremely low or undetectable in human plasma even after administration of very high doses (Gota et al. 2010; Cuomo et al. 2011).

Previously, we formulated a monoolein (MO)-based liquid crystalline nanoparticle dispersion loaded with curcumin and found that these nanoparticles showed a stable size and surface charge evolution (Baskaran et al. 2014). In another study, we found that the MO in the liquid crystalline nanoparticle dispersion was cytotoxic at concentrations $\geq$20 μg/mL (Madheswaran et al. 2015). The aim of the present study was to prepare NLC containing curcumin using phospholipid and fat as the lipid carriers in order to avoid the toxicity associated with MO. This approach encountered an unexpected obstacle relating to the stability of the nanoparticle dispersion: during extened storage, coalescence of the nanoparticles and curcumin crystal formation were observed.

Steroids such as cholesterol and ergosterol have a well-characterized ability to stabilize phospholipids in the cell membrane of eukaryotic cells. We therefore hypothesized that ginsenoside, a steroid glycoside, could play a role in the modification of NLC dispersion system consisted of phospholipids/fats and could increase the stability and bioavailability of the bioactives entrapped. Exert beneficial effect on the stabilization of the lipid carrier matrices which are composed of phospholipids/fats and are prone to problems associated with stability during the storage period.

The main aims of the present study were to investigate the effect of ginsenoside on coalescence and curcumin crystal formation within the phospholipid/fat-based NLC dispersion. The bioavailability of curcumin delivered using ginsenoside-modified NLC (G-NLC) was also investigated in rats.

Materials and methods

Materials

Curcumin was purchased from Sigma-Aldrich (St Louis, USA). Phosphatidylcholine (Phosal 53MCT) and lysophosphatidylcholine (Lipoid R LPC 20, LPC) were obtained from Lipoid (Germany). Refined hydrogenated soybean oil (HBO) was purchased from Lotte Foods (Seoul, Korea). Ginsenoside was prepared by fermentation of ginseng saponin obtained from The Zone PHC (Korea) for 7 days using *Saccharomyces cerevisiae* and a subsequent purification procedure. The ginsenosides present in the fermented ginseng saponin were composed of ginsenoside Rg1, 39.99%; Rd, 14.05%; F2, 13.79%; protopanaxadiol 11.55%; Rg3, 7.95%; compound K, 5.75%; protopanaxatriol, 1.83% and other minor components. All other chemicals were of reagent grade and used without further purification.

Preparation of G-NLC dispersion

The G-NLC dispersion was prepared by melt emulsification technique as described elsewhere with slight modification. Briefly, entire mixture of the ingredients specified in Table 1 was put into a round bottom flask and solubilized using magnetic stirrer at 60 °C. When the entire mixture was transparently solubilized, the ethanol was evaporated using rotary evaporator at 60 °C. The amount of ethanol evaporated was measured by weight difference. When the ethanol had been completely evaporated, preheated distilled water (60 °C) was added and the mixture was homogenized using IKA homogenizer at 24,000 rpm for 5 min. The resultant G-NLC dispersion was then cooled to room temperature and stored in the refrigerator (4 °C) until evaluation.

Characterization of G-NLC dispersion

The particle size distribution and polydispersity index (PDI) of the G-NLC dispersion were determined by dynamic light scattering using Zetasizer Nano S90 (Malvern Instruments, UK) at fixed angle of 90°. Zeta potential was measured using an electrophoretic light scattering method (Photal ELSZ-1000) at 25 °C, and the mean of three measurements was used.

Stability of the different G-NLC dispersion was evaluated in terms of physical stability during twelve months storage period in the refrigerator. Physical stability tests included changes in particle size, surface charge, and morphology of the G-NLC. Morphology of the G-NLC was assessed by a microscope (Olympus BX53 at ×400 magnification) to observe crystal formation. The morphology was further examined by TEM (JEM-2100F, Japan). A drop of diluted G-NLC dispersion was placed on carbon-coated copper grid and excess dispersion was removed with filter paper after 5 min. One drop of 2% phosphotungstic acid solution was added to enhance the contrast by negative-staining the nanoparticles, followed by air-drying at room temperature for 5 min. TEM images were taken at an accelerating voltage of 100 kV.

Table 1 Composition of ginsenoside-modified NLC dispersion

Composition code	Ginsenoside (g)	Curcumin (g)	Phosal 53 MCT (g)	LPC (g)	HBO (g)	Ethanol (g)	Distilled water (g)	Total (g)
NLC	–	0.1	2.0	0.2	0.2	1.0	27.5	30.0
G-NLC 100	0.1	0.1	2.0	0.2	0.2	1.0	27.4	30.0
G-NLC 200	0.2	0.1	2.0	0.2	0.2	1.0	27.3	30.0
G-NLC 300	0.3	0.1	2.0	0.2	0.2	1.0	27.2	30.0
G-NLC 400	0.4	0.1	2.0	0.2	0.2	1.0	27.1	30.0
G-NLC 500	0.5	0.1	2.0	0.2	0.2	1.0	27.0	30.0

G-NLC ginsenoside-modified nanostructured lipid carrier containing curcumin, *HBO* hydrogenated soybean oil, *LPC* lysophosphatidylcholine

Entrapment efficiency (EE) of the G-NLC dispersion was evaluated by centrifugation method as described elsewhere (Baskaran et al. 2014; Vijayakumar et al. 2017). The G-NLC dispersion (0.5 mL) was centrifuged at $4000 \times g$ for 30 min at 4 °C using Amicon Ultra-4 Filter Unit (MWCO 10,000 g/mol). Unentrapped (free) curcumin was separated from the G-NLC dispersion by centrifugation. Total amount of curcumin in the dispersion was measured using HPLC after destruction of the G-NLC dispersion by dilution with methanol (×20). EE was calculated by the following equation: $EE\ (\%) = 100 \times (D_{total} - D_{unentrapped})/D_{total}$, where D_{total} and $D_{unentrapped}$ are the amount of total and unentrapped curcumin in the G-NLC dispersion, respectively.

Differential scanning calorimetry (DSC) analysis was performed using Perkin Elmer DSC 8000 Series calorimeter (Waltham, USA). NLC dispersion was freeze-dried and used for DSC and X-ray diffraction (XRD) analyses. About 5 mg of each sample was loaded in an aluminum pan and hermetically sealed, and thermal behavior was assessed in the range of 30–230 °C at a scan rate of 20 °C/min with nitrogen gas flow rate of 20 mL/min. XRD was performed with Rigaku diffractometer using Cu Kα ($\lambda = 1.54$ Å) at a scanning angle from 5° to 50°. Scanning rate was 5°/min. For physical mixture, ginsenoside, curcumin, phosphatidylcholine, LPC, and HBO were mixed together in the mortar for comparison.

In vitro release of curcumin from G-NLC was evaluated by dialysis method as described previously (Baskaran et al. 2014). Briefly, G-NLC dispersion was 10-times diluted with distilled water and 1-mL of the diluted dispersion was sealed inside the dialysis bag (Spectra/Por® MWCO 12–14 kDa, USA) and placed into 20 mL of release medium with gentle shaking at 50 strokes/min in water bath at 37 °C. The release media used were simulated gastric fluid and intestinal fluid specified in USP 40 (pH 1.2 and 6.8, respectively) containing 0.5% w/v Tween 80. The whole medium was withdrawn at predetermined time intervals (1, 2, 3, 4, 5, 6 h) and replaced with fresh medium to make sure sink condition. Curcumin and Longvida™ dispersed in each release medium were used as control. The medium withdrawn was then analyzed for curcumin concentration using HPLC. Each experiment was performed in triplicate.

Pharmacokinetic study of G-NLC dispersion

Male Sprague–Dawley rats weighing 250 ± 20 g were purchased from OrientBio (Seoul, Korea) and acclimated for one week prior to experiment. All animal care and procedures were conducted according to the Guidelines of Center of Animal Care and Use (CACU) in Lee Gil Ya Cancer and Diabetes Institute, Gachon University, Korea. Eighteen rats were randomly assigned to two test groups and a control group and fasted for 12 h prior to the experiments. The rats had free access to water. The rats in the two test groups were orally administered with the G-NLC 500 dispersion (corresponding to 50 or 100 mg/kg curcumin) and the control group received 100 mg/kg pure curcumin dispersed in distilled water. Blood samples of 0.3 mL were serially withdrawn under anesthesia via subclavian vein into small heparinized Eppendorf tubes at 0.5, 1, 1.5, 2, 3, 4, and 8 h after administration. The blood samples were immediately centrifuged at 4,000 rpm for 15 min, and the plasma was isolated and stored at −20 °C until LC/MS assay. Pharmacokinetic parameters were evaluated using WinNonlin software (version 2.1).

HPLC and LC–MS/MS analyses

For in vitro experiment, curcumin was determined by HPLC system (Shimadzu, Japan) equipped with LC 20AD pump and SPD 20A UV–VIS detector at 400 nm. Column temperature was set at 25 °C. The column used was Phenomenex ODS-3 (4.6 × 150 mm) and mobile phase consisted of acetonitrile and 2% acetic acid (70:30 v/v). Quercetin was used as internal standard and the injection volume was 20 µL with flow rate of 0.4 mL/min. HPLC validation was performed by repeating five times a day for five consecutive days in the range of 50–2000 ng/mL curcumin.

For in vivo bioavailability study, curcumin was determined by LC–MS/MS system comprised of Agilent LC 1100 series (Agilent Technologies, CA, USA) binary pump, vacuum degasser and auto-sampler system connected to a 6490 triple quadrupole MS equipped with electrospray ionization (ESI) source with Agilent jet stream technology. Chromatographic separation was performed on a Zorbax Extend-C18 column (1.0 × 150 mm, 3.5 μm). The column temperature was maintained at 28 °C, and the auto-sampler temperature was set at 4 °C. Sample solutions (4 μL) were injected and the analytes were eluted using 0.1% formic acid in acetonitrile and 0.1% formic acid in water (50:50 v/v) at a flow rate of 0.1 mL/min. The isocratic separation run time was 10 min. Hesperetin was used as an internal standard. Curcumin and hesperetin were monitored using an API3000 mass spectrometer equipped with an ESI quadrupole mass analyzer. The operational parameters were as follows: argon as collision gas, gas flow at 14 L/min, source temperature at 250 °C, and collision energies of 14 and 24 eV for curcumin and hesperetin, respectively.

Quantification was performed using multiple reaction monitoring method with the precursor-to-product ion transition of 369.1 → 285.1 m/z for curcumin and 303.1 → 153 m/z for hesperetin. Mass data were collected and processed using the Mass Hunter QQQ Qualitative and Quantitative software (version B.04.00, Agilent Technologies, USA).

Calibration standards, quality control samples, and rat plasma samples were extracted by protein precipitation using acetonitrile. Prior to the analysis, each plasma sample was thawed to room temperature. A volume of 10 μL acetonitrile with standard working solution were added to 100 μL final volume of plasma sample in a 1.5 mL eppendorf tube. Then 200 μL acetonitrile with internal standard (5 ng/mL) was added for protein precipitation after vortexing for 1 min followed by centrifugation at 14,000 rpm for 15 min at 4 °C. The supernatant was separated and transferred to auto-sampler vial insert and 4 μL of the sample was injected into the LC–MS/MS system. The lower limit of quantification for curcumin was 1 ng/mL.

Statistical analysis

All data were analyzed by one-way ANOVA. Data are presented as mean ± standard deviation. A value of $p < 0.05$ was considered statistically significant.

Results

Six different NLC dispersions were prepared by melt emulsification technique using lipid carriers (Phosal 53 MCT, LPC, HBO) and ginsenoside as shown in Table 1. All the NLC dispersions were non-viscous opaque liquid with thick mango-yellow color. The mean particle size was in the range of about 300–500 nm. The particle size of the G-NLC 500 dispersion was significantly smaller than that of all other compositions tested (Table 2). All the six compositions showed PDI less than 0.3 as measured by dynamic light scattering, indicating homogeneous particle size distribution regardless of whether ginsenoside was added to the composition. The EE of curcumin was almost a hundred percent, and this was independent of the ingredients used in the NLC. Zeta potentials ranged from −29 to −32 mV for all compositions, indicating that ginsenoside caused a slight change in the potential of the nanoparticles.

Curcumin crystal formation was observed by microscopy at 400× magnification over 12 months. NLC dispersion prepared without ginsenoside rapidly showed needle-like crystals of curcumin. This was observed as early as during the homogenization process, with more than 10 crystals present in the observation field (Table 3). Furthermore, the needle-like crystals aggregated within one day and developed into hedgehog-like (radial direction) or hair-like (longitudinal direction) formations (Fig. 1). In contrast, crystal formation was delayed in NLCs prepared with ginsenoside, and no subsequent aggregation of the crystals was observed. Notably, the G-NLC 500 dispersion showed only a few crystals after storage at 4 °C for 12 months.

Particle size of the NLC dispersion increased during storage at 4 °C. The mean particle size of NLCs prepared in the absence of ginsenoside increased significantly, reaching beyond a micron at three months (Fig. 2). The mean particle sizes of the G-NLC 100/200/300 dispersion also showed greater than a micron at three months at 4 °C. Notably, however, G-NLC 400/500 preparations were still nanoparticles (submicron size) up to 12 months. This result was consistent with our microscopic observation of crystal's radial and/or longitudinal gathering in the G-NLC dispersion prepared with low amount of ginsenoside. Surface charge evolution showed slight fluctuation (±10 mV) during the 12 months. Although not significant, NLC dispersions with more amount of ginsenoside exhibited less fluctuation of the zeta potential (Fig. 2).

The TEM image revealed discrete and monodispersed nanoparticles with core/shell structure (Fig. 3). An additional layer resembling a corona was present in G-NLCs. The size of the nanoparticles in the TEM image was in agreement with the dynamic light scattering characterization. No shell layer was identified in the TEM image of NLCs prepared in the absence of ginsenoside.

DSC thermogram showed sharp endothermic peaks for curcumin at 181.9 °C, corresponding to its melting point and reflecting its crystalline nature (Fig. 4). The absence of an endothermic peak at this temperature in the G-NLC 500 composition confirmed the conversion of this crystalline nature to a molecularly dispersed amorphous state within the

Table 2 Characterization of ginsenoside-modified NLC dispersion

Composition code	Size (nm)	PDI	Zeta potential (mV)	EE (%)
NLC	469.0 ± 68.3	0.131 ± 0.134	−29.36 ± 0.54	99.96 ± 0.01
G-NLC 100	450.9 ± 40.4	0.217 ± 0.14	-30.60 ± 0.82	99.91 ± 0.01
G-NLC 200	464.9 ± 92.3	0.168 ± 0.10	-30.67 ± 0.91	99.99 ± 0.01
G-NLC 300	446.2 ± 63.4	0.147 ± 0.095	-31.05 ± 1.43	99.98 ± 0.01
G-NLC 400	372.0 ± 34.0	0.270 ± 0.198	-31.97 ± 1.40	99.97 ± 0.01
G-NLC 500	320.7 ± 19.6*	0.197 ± 0.038	-32.02 ± 1.09	99.99 ± 0.01

EE entrapment efficiency, *G-NLC* ginsenoside-modified nanostructured lipid carriercontaining curcumin, *PDI* polydispersity index

* $p < 0.05$ compared to other compositions

Table 3 Crystal formation of ginsenoside-modified NLC during storage period in refrigerator

Composition code	Storage period (months)							
	0	1	2	3	4	5	6	12
NLC	++	+++	+++	+++	+++	+++	+++	+++
G-NLC 100	–	+	++	++	+++	+++	+++	+++
G-NLC 200	–	+	++	++	++	+++	+++	+++
G-NLC 300	–	+	+	++	++	++	++	+++
G-NLC 400	–	–	–	–	–	+	+	++
G-NLC 500	–	–	–	–	–	–	–	+

G-NLC ginsenoside-modified nanostructured lipid carrier containing curcumin, – none, + minimal (<5 crystals in high power field), ++ moderate (5–10 crystals in high power field), +++ significant (>10 crystals in high power field)

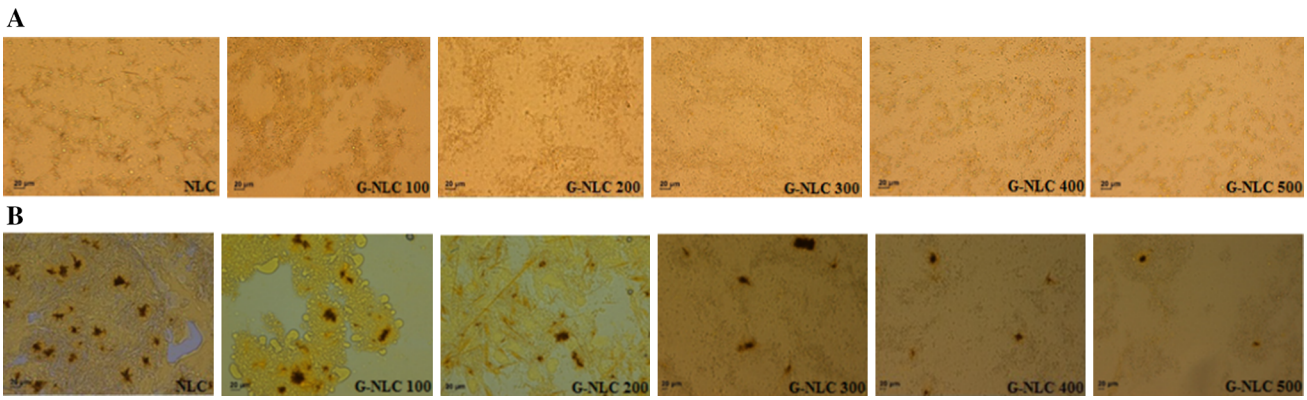

Fig. 1 Morphology evolution of ginsenoside-modifiedNLC during storage period in refrigerator. *G-NLC* ginsenoside-modified nanostructured lipid carrier containing curcumin. Microscopic images were taken at **a** zero day, **b** 12 months

nanoparticle infrastructure. This finding is also in agreement with the results for EE study which demonstrated almost 100% entrapment of curcumin within the NLC. The EE would be unlikely to reach this level unless curcumin was molecularly dispersed within the NLC. Physical mixture was also devoid of the endothermic peak because curcumin was solubilized into Phosal 53MCT during the trituration. XRD pattern of curcumin and HBO showed distinct sharp peaks while the peaks disappeared in G-NLC 500 (Fig. 4). This further confirmed that curcumin was molecularly dispersed in the lipid carrier matrix of the NLC.

Figure 5 illustrates the in vitro release profile of curcumin from different NLC dispersion. Curcumin release was slightly faster in pH 1.2 compared to pH 6.8 and it showed linear release pattern after lag time of 1 h. The G-NLC dispersions exhibited markedly faster release compared to the control and NLC ($p < 0.01$) in both pH condition. G-NLC dispersions prepared with more ginsenoside showed faster release than those prepared using less or no ginsenoside. Notably, in terms of the amount of curcumin released, G-NLC 400 and G-NLC 500 were far superior to Longvida.

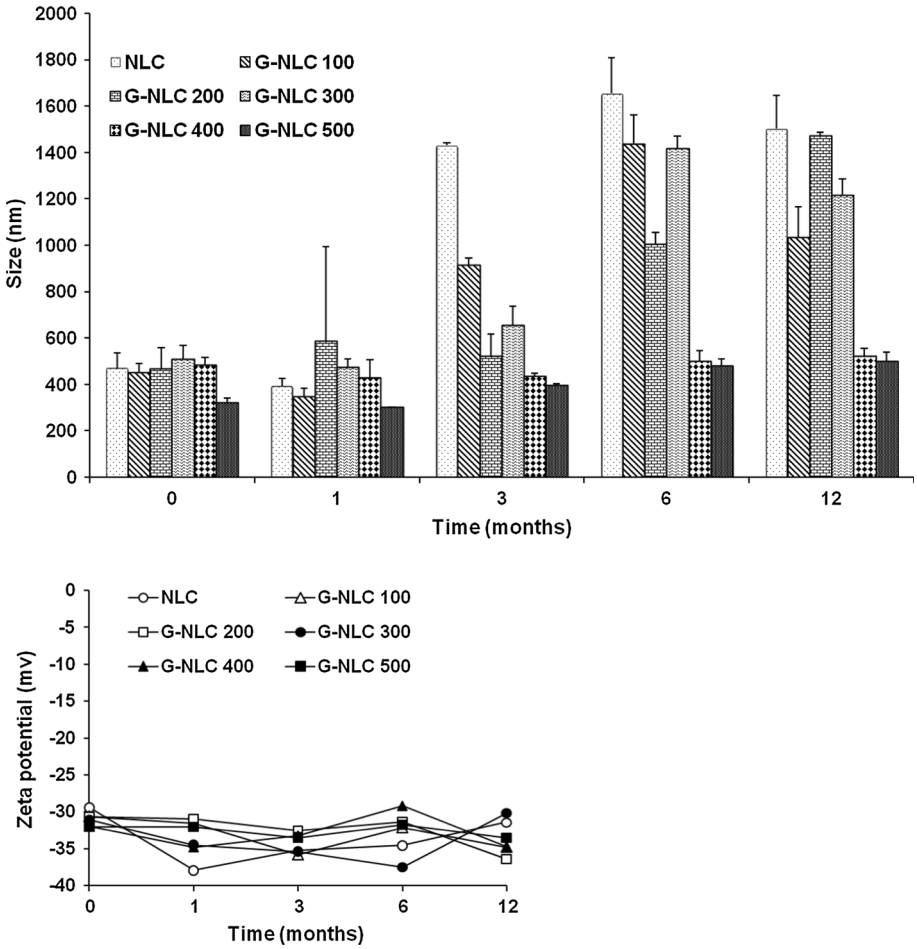

Fig. 2 Particle size and surface charge evolution of ginsenoside-modified NLC during storage period in refrigerator. *G-NLC* ginsenoside-modified nanostructured lipid carrier containing curcumin. Each value represents the mean ± SD (n = 3)

Figure 6 shows plasma level of free curcumin after oral administration of the G-NLC 500 dispersion to rats. No free curcumin was detected in the plasma of rats administered with pure curcumin dispersed into distilled water. In contrast, the plasma level of free curcumin increased dose-dependently following the administration of G-NLC 500. The maximum plasma level (C_{max}) was 15.2 and 32.3 ng/mL at doses of 50 and 100 mg/kg, respectively (Table 4). Time to reach maximum plasma level (T_{max}) was 30 min for both doses. Although not obvious, the plasma level of curcumin rose up again at 3 h after administration, suggesting enterohepatic circulation. Area under the curve up to 8 h ($AUC_{0–8}$) was 18.47 and 74.09 h ng/mL at doses of 50 and 100 mg/kg, respectively.

Discussion

There has been extensive research on the pharmacological activities of curcumin, and it is being widely used in Indian medicine for diverse disorders (Sinha et al. 2003; Kulkarni and Dhir 2010). Recently, curcumin found its use in the treatment of cancer as an alternative medicine because it was able to kill cancer cells without affecting normal cells (Karunagaran et al. 2005; Ravindran et al. 2009). However, the benefit in real practice is very limited due to concerns on its poor solubility (2.7 ± 0.2 μg/mL) and bioavailability. Incorporation of curcumin into nanoparticle delivery system is an attractive methodology to overcome these hurdles (Maiti et al. 2007; Khalil et al. 2013). In this study, we incorporated curcumin into the phospholipid-based NLC and found that the solubility was improved more than 4600 times (12450.4 ± 105.3 μg/mL).

However, in the preparation of the NLC dispersion, we faced unexpected problems, which were aggregation of the nanoparticles and curcumin crystal formation during the storage. To address these problems, we tried several additives such as Tween and Span series surfactants (20, 40, 60, and 80), cholesterol oleate, and various bile salts to resolve the problems. However, all the trials using these additives did not succeed in resolving the problems. As another attempt, we used ginsenoside expecting that its steroid-like molecular structure could exert beneficial effect on the inhibition of coalescence of the phospholipid/fat-based nanoparticles just as cholesterol contributes to the stabilization of cell membranes phospholipids.

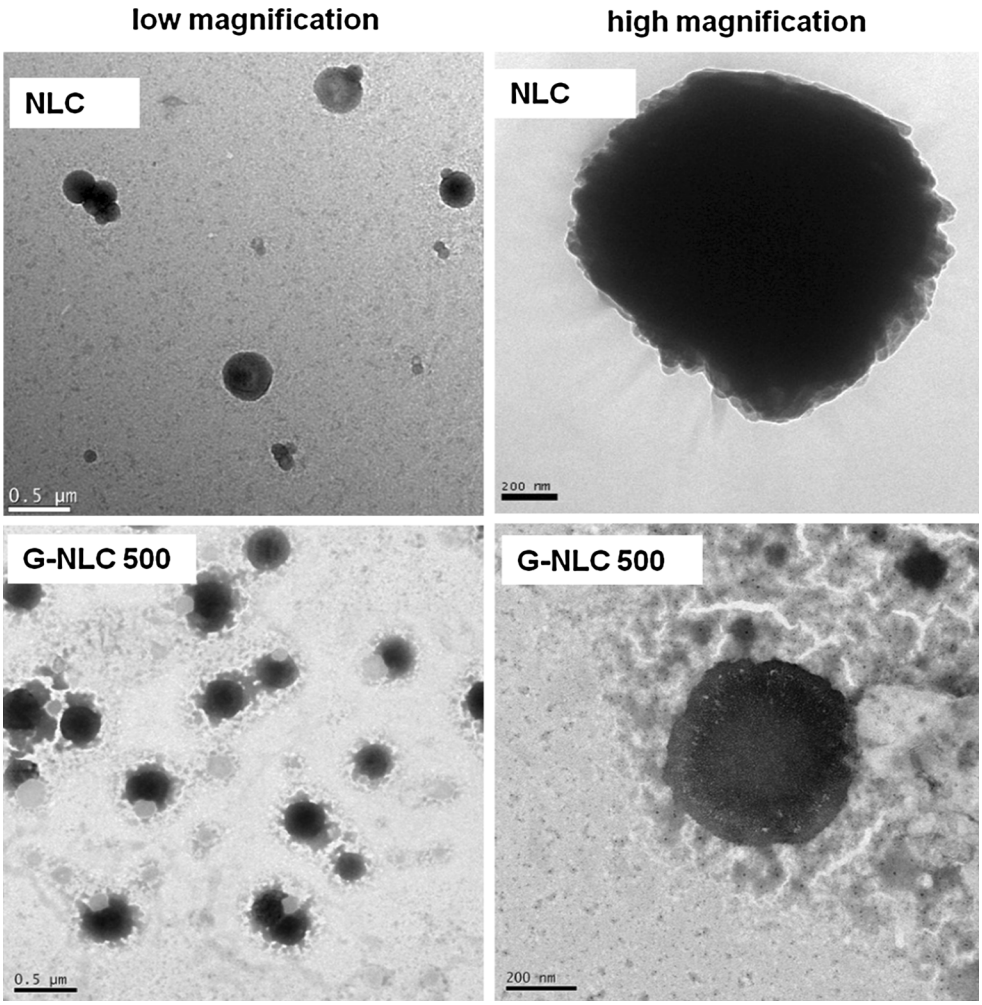

Fig. 3 TEM images of ginsenoside-modified NLC. *G-NLC* Ginsenoside-modified nanostructured lipid carrier containing curcumin, *TEM* transmission electron microscopy

Preparation of NLC dispersions using ginsenoside successfully inhibited curcumin crystal formation both immediately after preparation and during an extended storage period for up to 12 months (Table 3; Fig. 1). This is the first report of the use of ginsenoside as a pharmaceutical excipient to resolve problems associated with solubility and stability, especially for long term stability of a nanoparticle system. Although the mechanism underlying this inhibition has not yet been elucidated, it is clear that ginsenosides affected the solubilization of curcumin and/or modulated the lipid carrier matrix of the NLC so that curcumin molecules did not diffuse out of the nanoparticles. Chemical stability of curcumin was also significantly improved with >90% remaining after 12 months at 4 °C for G-NLC 400 and G-NLC 500.

The addition of ginsenoside resulted in smaller particles with more homogeneous size distribution (Table 3). Ginsenoside caused a slight change in the zeta potential of the nanoparticles, indicating modulation of the lipid carrier matrix, specifically on the charge-bearing head moiety of the phosphatidylcholine molecules (Table 2). Ginsenoside also inhibited size evolution of the nanoparticles during storage. Notably, when the ratio of ginsenoside to lipid carrier matrix was beyond 15% (G-NLC 400/500 dispersions), there was no size evolution during storage for up to 12 months (Fig. 2). Limitation of this study is that NLC dispersion was stored in refrigerator so stability at room temperature might be shorter than the findings in this study. Colloidal dispersions with higher zeta potential (negative or positive) were reported to show increased resistance to coagulation or flocculation during storage (Greenwood and Kendall 1990; Hanaor et al. 2012). The addition of ginsenoside only resulted in a subtle change in zeta potential of about 2 mV in the present study, implying that other mechanisms might also have contributed to the enhanced long-term stability of the G-NLC dispersions.

We investigated the nanoparticle structure using TEM in order to identify any plausible mechanism for the enhanced

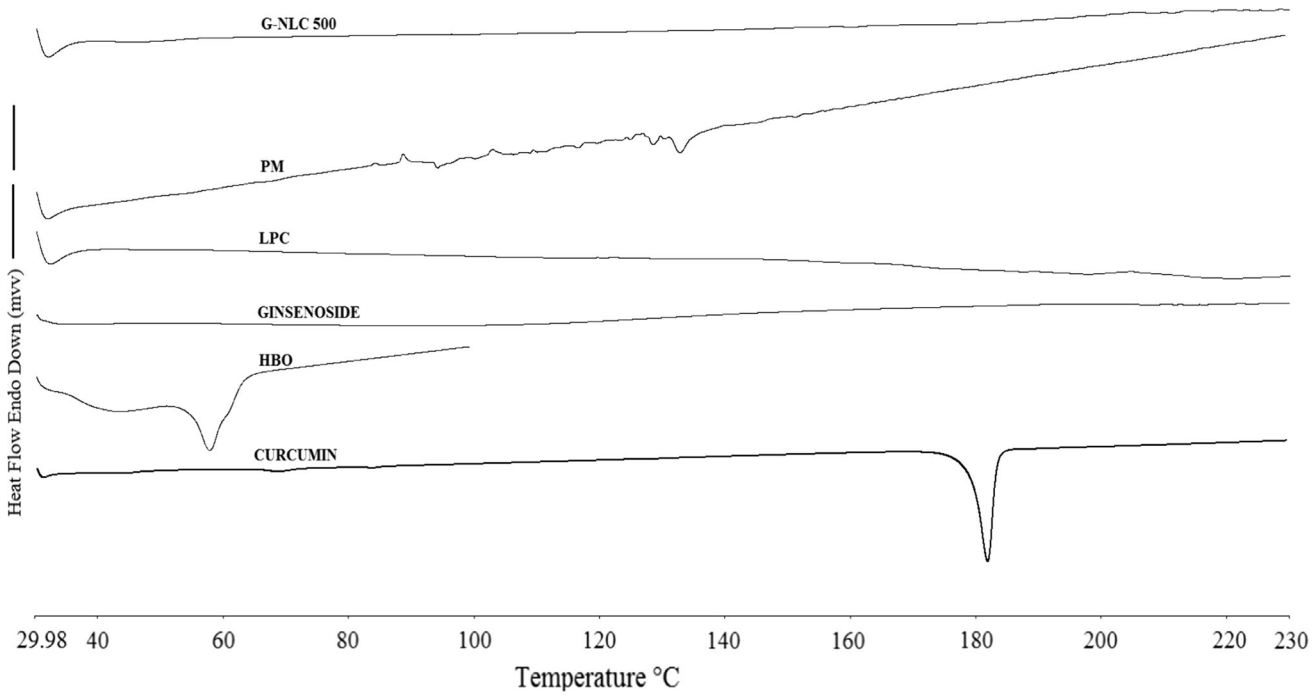

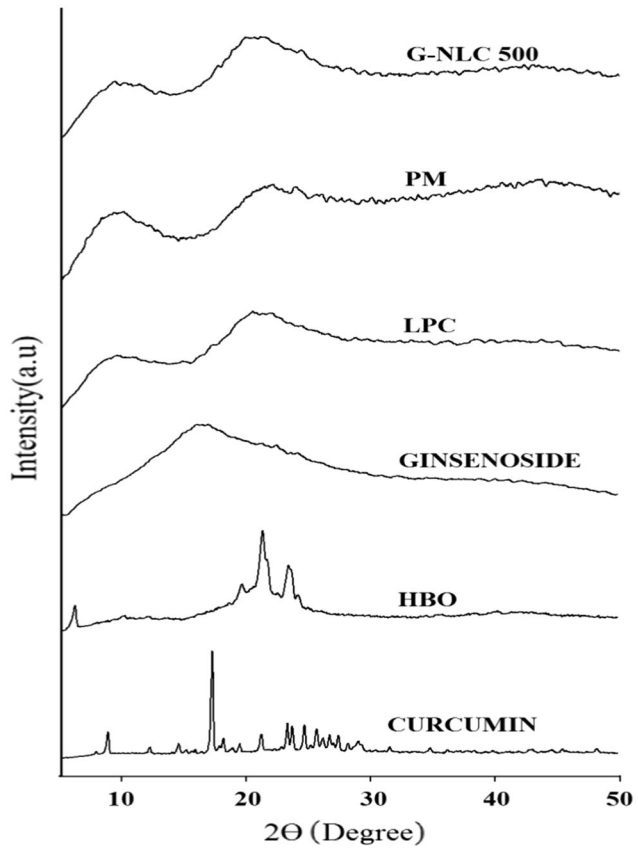

Fig. 4 DSC thermograms and XRD patterns of ginsenoside-modified NLC, each ingredient, and its physical mixture. *DSC* differential scanning calorimetry, *G-NLC* ginsenoside-modified nanostructured lipid carrier containing curcumin, *HBO* hydrogenated soybean oil, *LPC* lysophosphatidylcholine, *PM* physical mixture, *XRD* X-ray diffraction

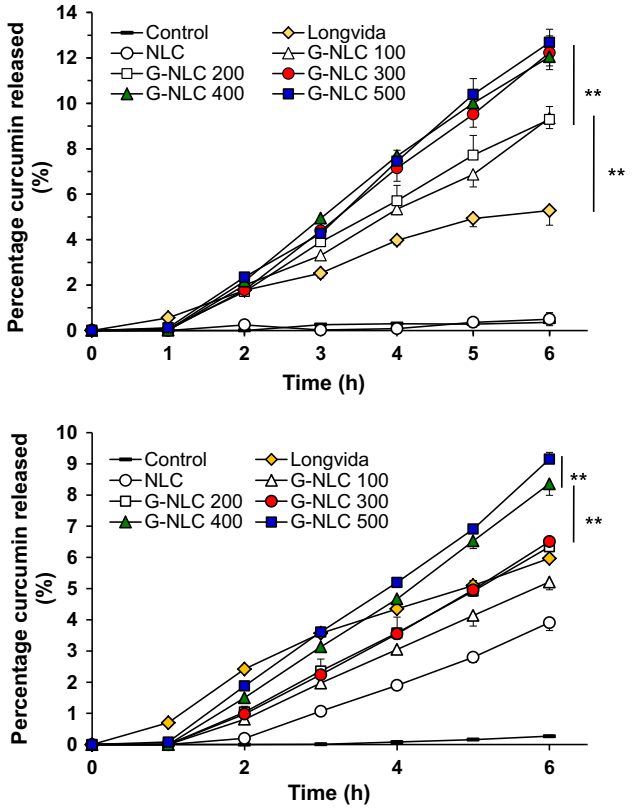

Fig. 5 In vitro release of curcumin from ginsenoside-modified NLC. *G-NLC* ginsenoside-modified nanostructured lipid carrier containing curcumin (*top panel* in simulated gastric fluid at pH 1.2, *bottom panel* in simulated intestinal fluid at pH 6.8). Each value represents the mean ± SD (n = 3). ** $p < 0.01$

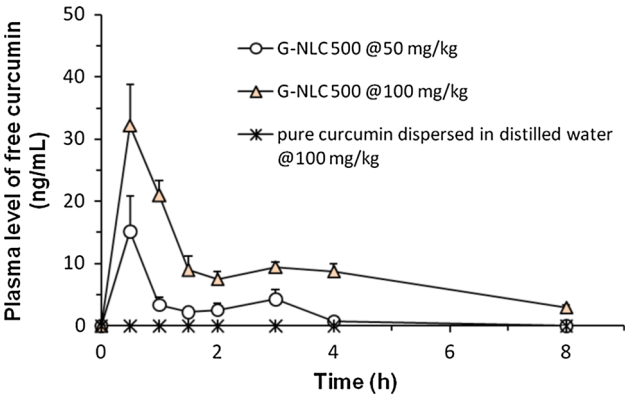

Fig. 6 Plasma level of free curcumin after oral administration of ginsenoside-modified NLC to rats. G-NLC: Ginsenoside-modified nanostructured lipid carrier containing curcumin. Each value represents the mean ± SD (n = 6)

long-term stability. TEM imaging of the G-NLC 500 dispersion showed core and shell layer. Furthermore, higher magnification of these nanoparticles revealed that the shell layer was surrounded by an irregular dendrimer-like corona. The core and shell layer appeared to be composed of fats and phospholipids, respectively. Since ginsenosides have relatively low molecular weight (<1000 g/mole) and sugar molecule(s) attached to their steroid skeleton, they are amphiphilic substance in nature. Rg1 and F2 constituted more than half (53.78%) of the ginsenosides used in this study, and they have two glucose molecules attached on the steroid skeleton. The preferred placement of the ginsenosides in the nanoparticle is thus presumed to be at the interfacial area between the hydrophobic lipid carrier matrix and the hydrophilic aqueous environment. Inclusion of ginsenoside molecules in the outer layer of the nanoparticles would protect them from direct contact with each other. This would therefore significantly reduce nanoparticle aggregation. TEM imaging and the significant inhibition of particle size evolution found in G-NLC 400/500 dispersion provided evidence for the blocking the collision of the nanoparticles with each other (Fig. 2). Therefore, it seems very reasonable to presume that the ginsenoside molecules are placed in the dendrimer-like corona of the nanoparticles.

Our pharmacokinetic study of the G-NLC 500 dispersion in rats found that free curcumin (unmetabolized) level in the plasma increased in a dose-dependent manner following oral administration. The major metabolites of curcumin identified by other researchers were conjugates of glucuronide and sulfate (Vareed et al. 2008). It is noteworthy that the "free form" of curcumin is responsible for the anticipated health benefit of curcumin, and the AUC of the free curcumin is practically zero or extremely low. Asai and Miyazawa reported that C_{max} of free curcumin was less than 1.8 ng/mL in rats following oral administration of 100 mg/kg (Asai and Miyazawa 2000). Based on the C_{max} comparison (because these authors did not provide AUC value), C_{max} of the parent curcumin in our result represents 17.9 times greater than their result. The mechanism underlying this remarkable improvement may relate to the nature of the nanoparticles employed, reflecting the incorporation of ginsenosides into the lipid carrier matrix. Release of curcumin at the right time in the upper alimentary tract may also be a contributor for the improved absorption. Another possibility might be that ginsenoside facilitated endocytosis through enterocyte cell membrane. Cellular uptake study of the G-NLC nanoparticle is currently under investigation in our laboratory using human enterocytes and fluorescence microscopy.

We successfully developed stable NLC dispersion using ginsenoside as a pharmaceutical excipient. Ginsenoside played a key role in the inhibition of coalescence of these phospholipid/fat-based nanoparticles and of curcumin crystal formation in the NLC dispersions. Physicochemical and biological investigations performed in this study suggested that ginsenoside modulated the lipid carrier matrix of phospholipid/fat-based NLCs, extending their shelf-life and improving the bioavailability of their cargo in rats.

Table 4 Maximum plasma level of free curcumin and area under the curve after oral administration of ginsenoside-modified NLC to rats (n = 6)

Composition code	Dose (mg/kg)	T_{max} (h)	C_{max} (ng/mL)	AUC_{0-8} (h × ng/mL)	Elimination half-life (h)
G-NLC 500	50	0.5	15.2 ± 5.70	18.47 ± 6.87	2.24 ± 1.06
G-NLC 500	100	0.5	32.3 ± 6.55**	74.09 ± 14.26**	2.90 ± 1.12
Pure curcumin dispersed in distilled water	100	NA	Not detected	Not detected	NA

AUC_{0-8} area under the curve from zero to 8 h, *C_{max}* maximum plasma level of free curcumin, *G-NLC* ginsenoside-modified nanostructured lipid carrier containing curcumin, *NA* not applicable

** $p < 0.01$ compared to 50 mg/kg dose

These results strongly suggest that ginsenoside has considerable potential as a pharmaceutical excipient that increases the utility of various bioactives within pharmaceutical preparations.

Acknowledgements This study was supported by the Research Center Hospital Project in Gil Hospital, Gachon University (FRD2014-06-02).

Compliance with ethical standards

Conflict of interest The authors declare no conflicts of interest.

References

Anuchapreeda S, Fukumori Y, Okonogi S, Ichikawa H (2012) Preparation of lipid nanoemulsions incorporating curcumin for cancer therapy. J Nanotechnol 41:1–11

Arun G, Shweta P, Upendra KJ (2012) Formulation and evaluation of ternary solid dispersion of curcumin. Int J Pharm Pharm Sci 4:360–365

Asai A, Miyazawa T (2000) Occurrence of orally administered curcuminoid as glucuronide and glucuronide/sulfate conjugates in rat plasma. Life Sci 67:2785–2793

Baskaran R, Madheswaran T, Sundaramoorthy P, Kim HM, Yoo BK (2014) Entrapment of curcumin into monoolein-based liquid crystalline nanoparticle dispersion for enhancement of stability and anticancer activity. Int J Nanomed 9:3119–3130

Byeon SE, Choi WS, Hong EK, Lee J, Rhee MH, Park HJ, Cho JY (2009) Inhibitory effect of saponin fraction from codonopsis lanceolata on immune cell-mediated inflammatory responses. Arch Pharm Res 32:813–822

Cuomo J, Appendino G, Dern AS, Schneider E, McKinnon TP, Brown MJ, Togni S, Dixon BM (2011) Comparative absorption of a standardized curcuminoid mixture and its lecithin formulation. J Nat Prod 74:664–669

Du ZY, Wei X, Huang MT, Zheng X, Liu Y, Conney AH, Zhang K (2013) Anti-proliferative, anti-inflammatory and antioxidant effects of curcumin analogue A2. Arch Pharm Res 36:1204–1210

Goel A, Aggarwal BB (2010) Curcumin, the golden spice from Indian saffron, is a chemosensitizer and radiosensitizer for tumors and chemoprotector and radioprotector for normal organs. Nutr Cancer 62:919–930

Gota VS, Maru GB, Soni TG, Gandhi TR, Kochar N, Agarwal MG (2010) Safety and pharmacokinetics of a solid lipid curcumin particle formulation in osteosarcoma patients and healthy volunteers. J Agric Food Chem 58:2095–2099

Greenwood R, Kendall K (1990) Electroacoustic studies of moderately concentrated colloidal suspensions. Faraday Discuss Chem Soc 90:301–312

Hanaor DAH, Michelazzi M, Leonelli C, Sorrell CC (2012) The effects of carboxylic acids on the aqueous dispersion and electrophoretic deposition of ZrO_2. J Eur Ceram Soc 32:235–244

Karunagaran D, Rashmi R, Kumar TR (2005) Induction of apoptosis by curcumin and its implications for cancer therapy. Curr Cancer Drug Targets 5:117–129

Khalil NM, do Nascimento TC, Casa DM, Dalmolin LF, de Mattos AC, Hoss I, Romano MA, Mainardes RM (2013) Pharmacokinetics of curcumin-loaded PLGA and PLGA–PEG blend nanoparticles after oral administration in rats. Colloids Surf B Biointerfaces 101:353–360

Kim JS, Joo EJ, Chun J, Ha WW, Lee JH, Han Y, Kim YS (2012) Induction of apoptosis by ginsenoside Rk1 in SK-MEL-2-human melanoma. Arch Pharm Res 35:717–722

Kulkarni S, Dhir A (2010) An overview of curcumin in neurological disorders. Indian J Pharm Sci 72:149–154

Kumar SS, Mahesh A, Mahadevan S, Mandal AB (2014) Synthesis and characterization of curcumin loaded polymer/lipid based nanoparticles and evaluation of their antitumor effects on MCF-7 cells. Biochim Biophys Acta 1840:1913–1922

Madheswaran T, Baskaran R, Sundaramoorthy P, Yoo BK (2015) Enhanced skin permeation of 5α-reductase inhibitors entrapped into surface-modified liquid crystalline nanoparticles. Arch Pharm Res 38:534–542

Maiti K, Mukherjee K, Gantait A, Saha BP, Mukherjee PK (2007) Curcumin–phospholipid complex: preparation, therapeutic evaluation and pharmacokinetic study in rats. Int J Pharm 330:155–163

Menon VP, Sudheer AR (2007) Antioxidant and anti-inflammatory properties of curcumin. Adv Exp Med Biol 595:105–125

Piao XL, Wu Q, Yang J, Park SY, Chen DJ, Liu HM (2013) Dammarane-type saponins from heat-processed *Gynostemma pentaphyllum* show fortified activity against A549 cells. Arch Pharm Res 36:874–879

Popat A, Karmakar S, Jambhrunkar S, Xu C, Yu C (2014) Curcumin-cyclodextrin encapsulated chitosan nanoconjugates with enhanced solubility and cell cytotoxicity. Colloids Surf B Biointerfaces 117:520–527

Prasad S, Tyagi AK, Aggarwal BB (2014) Recent developments in delivery, bioavailability, absorption and metabolism of curcumin: the golden pigment from golden spice. Cancer Res Treat 46:2–18

Ravindran J, Prasad S, Aggarwal BB (2009) Curcumin and cancer cells: how many ways can curry kill tumor cells selectively? AAPS J 11:495–510

Sinha R, Anderson DE, McDonald SS, Greenwald P (2003) Cancer risk and diet in India. J Postgrad Med 49:222–228

Tabatabaei Mirakabad FS, Akbarzadeh A, Milani M, Zarghami N, Taheri-Anganeh M, Zeighamian V, Badrzadeh F, Rahmati-Yamchi M (2016) A comparison between the cytotoxic effects of pure curcumin and curcumin-loaded PLGA-PEG nanoparticles on the MCF-7 human breast cancer cell line. Artif Cells Nanomed Biotechnol 44:423–430

Udompornmongkol P, Chiang BH (2015) Curcumin-loaded polymeric nanoparticles for enhanced anti-colorectal cancer applications. J Biomater Appl 30:537–546

Vareed SK, Kakarala M, Ruffin MT, Crowell JA, Normolle DP, Djuric Z, Brenner DE (2008) Pharmacokinetics of curcumin conjugate metabolites in healthy human subjects. Cancer Epidemiol Biomark Prev 17:1411–1417

Vijayakumar A, Baskaran R, Jang YS, Oh SH, Yoo BK (2017) Quercetin-loaded solid lipid nanoparticle dispersion with improved physicochemical properties and cellular uptake. AAPS PharmSciTech 18:875–883

Wang W, Zhu R, Xie Q, Li A, Xiao Y, Li K, Liu H, Cui D, Chen Y, Wang S (2012) Enhanced bioavailability and efficiency of curcumin for the treatment of asthma by its formulation in solid lipid nanoparticles. Int J Nanomed 7:3667–3677

Zhang YX, Wang L, Xiao EL, Li SJ, Chen JJ, Gao B, Min GN, Wang ZP, Wu YJ (2013) Ginsenoside-Rd exhibits anti-inflammatory activities through elevation of antioxidant enzyme activities and inhibition of JNK and ERK activation in vivo. Int Immunopharmacol 17:1094–1100